

Title: Structural basis for pH-dependent retrieval of ER proteins from the Golgi by the KDEL receptor

Philipp Bräuer¹, Joanne L. Parker¹, Andreas Gerondopoulos¹, Iwan Zimmermann²,
Markus A. Seeger², Francis A. Barr^{1*}, & Simon Newstead^{1*}.

¹Department of Biochemistry, University of Oxford, South Parks Road, Oxford OX1 3QU.

² Institute of Medical Microbiology, University of Zurich, 8006 Zurich, Switzerland.

* simon.newstead@bioch.ox.ac.uk, francis.barr@bioch.ox.ac.uk

One Sentence Summary: Transporter-like architecture facilitates pH-dependent protein retrieval within the secretory pathway.

Abstract

Selective export and retrieval of proteins between the endoplasmic reticulum (ER) and Golgi is indispensable for eukaryotic cell function. An essential step in the retrieval of ER luminal proteins from the Golgi is the pH-dependent recognition of a C-terminal KDEL signal by the KDEL receptor. Here, we present crystal structures of the chicken KDEL receptor in the apo ER state, KDEL-bound Golgi state, and in complex with an antagonistic synthetic nanobody (sybody). These structures show a transporter-like architecture that undergoes conformational changes on KDEL binding, and reveal a pH-dependent interaction network crucial for recognition of the carboxy-terminus of the KDEL signal. Complementary in vitro binding and in vivo cell localisation data explain how these features create a pH-dependent retrieval system in the secretory pathway.

In eukaryotic cells, millimolar levels of chaperones required for protein folding in the endoplasmic reticulum (ER) are discriminated from newly synthesized secretory and membrane proteins which pass through the ER on their way to the Golgi (1). Luminal chaperones and ER-resident membrane proteins carry a carboxy-terminal Lys-Asp-Glu-Leu (KDEL) sequence required for retention in the ER (2). When these proteins escape to the Golgi, they are recognised by an integral membrane protein, the KDEL receptor (KDELR), and retrieved back to the ER (3). The retrieval receptor *ERD2* was discovered in 1990 as one of a number of ER retention defective (ERD) mutants in *Saccharomyces cerevisiae* (3-5). *ERD2* encodes the 26 kDa KDELR responsible for the ability of yeast to retain ER luminal chaperones (3). It is predicted to have seven transmembrane domains and forms part of a large and diverse family of membrane proteins called the PQ-loop superfamily, which play important roles in lysosomal transport, tissue development and nutrient transport in plants and bacteria (6). The KDELR is localised to the cis-Golgi where it can efficiently capture escaped ER luminal proteins (7, 8). The interaction with KDEL proteins is pH-sensitive, with maximal binding below pH 6 (9). The luminal pH of the cis-Golgi is 6.2, whereas the ER lumen is 7.2-7.4 (10, 11), explaining how the KDELR could bind and release KDEL carrying proteins in these organelles, respectively. Binding of a protein with a KDEL sequence to the receptor triggers incorporation of the complex into COPI vesicles resulting in its return back to the ER (12). Once there, the complex dissociates and the receptor is rapidly trafficked back to the Golgi via COPII vesicles (13, 14). The cytoplasmic surface of the KDELR is thought to mediate the interaction with the COPI vesicle machinery, although how this occurs or is coupled to KDEL binding remains unknown (13, 14). To elucidate the molecular basis for receptor-mediated retrieval in the secretory pathway, we determined the crystal structure of the KDELR in both the peptide free and bound states.

To determine the atomic structure of the KDELR, we screened several homologues from different eukaryotic sources to identify a receptor suitable for structural and biophysical characterisation. *Gallus gallus* KDEL2 displays the characteristic pH-dependent binding for the KDEL peptide in the absence of any additional cofactors, with a K_D of $1.25 \mu\text{M} \pm 0.14$ at pH 5.0 in detergent (Figure 1A). Binding of the peptide is calcium independent (Fig. S1), suggesting this plays no role in the retrieval cycle. The structure was determined to 2.5 Å resolution at pH 9.0, in the peptide free apo state (Table S1). The structure has similarities to the eukaryotic SWEET transporter (15) (Fig. S2), despite sharing only 24% sequence identity, and does not resemble the G protein coupled receptor (GPCR) family of cell surface receptors.

The receptor adopts a compact structure, consisting of 7 transmembrane (TM) alpha helices arranged loosely in a hexagon configuration when viewed from above (Figure 1B). The first three N- and last three C-terminal helices form two internal triple helix bundles arranged in a 1-3-2 sequence (THBs), connected with inverted topology by a linker helix TM4. This structural arrangement, whereby the THBs are inverted relative to each other by a pseudo two-fold rotation axis in the plane of the membrane (Fig. S3), suggests an evolutionary relationship to secondary active transporters (6).

The surface of the cytosolic face contains a prominent central band of negative charge running down the centre (Figure 1C). The negative charge is contributed by several acidic residues invariant in the mammalian KDELRs: Asp87, Glu143, Glu145 and the C-terminus of TM7 (Fig. S4 & S5). Cell biological studies identified these and several additional residues in the cytoplasmic portion of human KDELR (*ERD2.1*) that result in retention within the ER when mutated (16). Interestingly, many of these residues function to support the structural integrity of this electrostatic feature, suggesting this may form part of a di-acidic COPII-binding ER-exit motif (17). The hydrophobic surface of the receptor is noticeably short, measuring 27 Å at its widest point (Figure 1D), consistent with other membrane proteins resident in thin membrane bilayers of the ER and Golgi (18, 19). The asymmetric position of this narrow hydrophobic belt suggests that the receptor projects outward from the cytosolic side of the membrane, exposing the negative charged surface. Likewise, the receptor would be flush with the luminal side of the ER and Golgi membranes, where it recognises KDEL containing proteins. A large polar cavity is observed at the luminal side of the receptor, flanked by side chains from TMs 1-3 from the N-terminal THB and TMs 5-7 from the C-terminal THB and measuring 13 x 15 x 12 Å (Figure 1E). The electrostatic surface of the cavity is charged, having a pronounced dipolar character contributed by Arg5 (TM1) and Arg169 (TM6), which are positioned opposite Glu117 (TM5) and Asp177 (TM7) (Fig. S6). As discussed later, these residues form an integral part of the KDEL signal sequence recognition site.

Binding of the KDEL signal sequence to the human receptor is pH-dependent, yet the mechanism through which high affinity binding depends on acidic pH is unclear (9, 20). To address this question, we determined a second structure of the Gg KDELR2 bound to the Thr-Ala-Glu-Lys-Asp-Glu-Leu (TAEKDEL) peptide at an acidic pH of 6.0, to a resolution of 2.0 Å (Table S1). The TAEKDEL peptide bound in the luminal facing cavity adopts a vertical orientation with respect to the membrane and the Lys-Asp-Glu-Leu residues are clearly resolved in the electron density map (Figure 2A & Fig. S7). Compared to the apo form the peptide bound receptor shows rearrangement of the side chains and helices forming the luminal

facing cavity (Figure 2B & Fig. S8). The cytoplasmic half of TM6 rotates inwards, resulting in the movement of Arg159 ~ 4.8 Å towards the peptide. This allows the carboxy terminus of the KDEL ligand to be anchored in place through two salt bridge interactions to Arg159 (TM6) and Arg47 (TM2) (Figure 2B). In this conformation, the luminal half of TM1 has moved outwards to accommodate the peptide, with Arg5 adopting a new rotamer configuration to interact with a carbonyl group on the peptide. Movement of TM1 also creates a pocket that accommodates the leucine side chain of the KDEL sequence. Recognition of the remaining side chains is predominantly mediated through electrostatic interactions to the sides of the luminal facing cavity. The positive amine group of the lysine interacts with Glu117 (TM5) in a negatively charged pocket (Figure 2C). The aspartate of the KDEL sequence makes a salt bridge to Arg169 (TM6), whereas the glutamate interacts via a third salt bridge to Arg5 (TM1) and makes a hydrogen bond interaction to Trp166, which similarly to Arg159, moves inwards to engage the peptide during the movement of TM6. The KDELR shows maximal binding between pH 5.0-5.4 with a gradual reduction in affinity until pH 7.0 (Figure 1A). Our structures reveal that repositioning of TM6 upon peptide binding is stabilised through the formation of a short hydrogen bond, measuring ~ 2.5 Å between Tyr158 (TM6) and Glu127 (TM5) (Figure 2D & Fig. S9). Formation of this short hydrogen bond would stabilize the new position of TM6, locking the peptide in place through its interaction with Arg159. Tyr158 sits close to a strictly conserved histidine on TM1, His12, forming an aromatic interaction. Two water molecules sit at the bottom of the peptide binding site, coordinating the peptide carboxyl group to both Tyr158 and His12, which are further stabilised through a hydrogen bond to Asp9 on TM1 (Figure 2D & Movie S1). Given its solvent accessible position within the peptide binding site, it is possible that protonation of His12 facilitates the formation of the short hydrogen bond that stabilises the repositioning of TM6, and thus acts as the pH sensor within the receptor. Supporting this proposal, conservative mutations in these residues resulted in the loss of KDEL binding in vitro (Figure 3A). The loss of binding to the chicken receptor in vitro was matched by a failure of equivalent variants of the human receptor (ERD2.1) to respond to KDEL ligand overexpression in vivo, with the receptor remaining localised in the Golgi despite the presence of KDEL ligand (Figure 3B & 3C). Mutation of Arg159 (TM6) resulted in a ligand binding defective protein trapped in the ER (Figure 3A-3C), suggesting this residue is important for the conformational stability of the receptor.

In the peptide-bound structure, we also observed a pronounced effect at the cytoplasmic surface of the receptor, with TM7 moving ~ 14 Å away from TM5, relative to the apo receptor and creating a new cavity facing the cytoplasm (Figure 4A & 4B). This movement results in

the repositioning of a strictly conserved acidic residue, Asp193 (TM7). Although an Asp193 to Asn mutant in the human receptor was previously shown to bind KDEL peptide *in vitro* (16), our data show this variant remains trapped in the Golgi *in vivo*, even in the presence of an excess of KDEL ligand (Figure 4C & 4D). This supports the view that movement of TM7 and opening of the cytosol facing cavity is important for ER retrieval via COPI. Consistent with this hypothesis, the movement of TM7 exposes a cluster of lysine residues Lys201, 204 & 206 buried in the apo receptor (Fig. 4A), that could form an ER-retrieval motif (21, 22). Additionally, the movement of TM6, discussed in relation to peptide binding above, causes the peptide chain linking TM5 and TM6 to shorten, as the length of TM6 is extended by one helical turn at the cytoplasmic end (Fig. S10). This rearrangement results in the central band of negative charge, which was a prominent feature of the cytoplasmic face of the apo receptor, to lengthen and split into two equal regions (Figure 4C). It is likely such a drastic change in the electrostatics on the cytosolic facing surface of the receptor plays a role mediating the interaction between the KDEL receptor and the COPI and COPII coatamer complexes during receptor trafficking. As already noted, the exposed lysine cluster on TM7 is similar to previously observed KKXX and KxKXX di-lysine motifs, which are important in COPI-dependent Golgi to ER transport (21, 22). To test their importance in the human KDEL receptor, we mutated this motif and observed the protein remained localised in the Golgi upon KDEL ligand overexpression (Figure 4D & 4E). This motif therefore plays an important role during KDEL-mediated ER retrieval.

In the course of determining the crystal structure, we employed single domain antibodies, or sybodies, generated using an *in vitro* selection platform (23). A crystal structure, obtained at 2.23 Å resolution in the absence of KDEL peptide (Table S1), demonstrates that the CDR3 loop of the sybody binds within the luminal facing cavity, yet fails to induce either the movement of TM6 or TM7 (Fig. S11A-E). Using a version of Syb37, targeted to the Golgi lumen, Syb37^{Sec}, we observed partial redistribution of KDEL receptor-Syb37^{Sec} complexes from the Golgi to LAMP1-positive structures (Fig. S11F). These results are consistent with the receptor no longer undergoing normal signal mediated retrieval from the Golgi, but instead following the bulk flow pathway to the lysosome. Importantly, Syb37^{Cyto}, a cytoplasmic version unable to access the Golgi lumen, did not have this effect. The inability of the sybody to activate the KDEL receptor either *in vitro* or *in vivo* highlights the importance of the specific interactions made to the peptide in the luminal facing cavity, and subsequent movements in TM6 and TM7, that we propose define two conformations of the KDEL receptor, which are important for anterograde and retrograde trafficking respectively.

Taken together, our data support a mechanism whereby changes in the electrostatics on the cytoplasmic surface of the receptor, in combination with protonation of a key histidine following peptide binding, play an important role in ER retrieval of the receptor via the COPI pathway (Fig. S11). An important discovery from this work is the presence of mutually exclusive basic COPI and putative acidic patch COPII recognition motifs. TM7 plays a pivotal role in presenting these motifs. The structural change in TM7 is stabilised by an interaction network involving a conserved histidine located adjacent to the KDEL signal sequence binding pocket. This creates an elegant way for the KDEL receptor to switch between the COPII ER to Golgi and COPI Golgi to ER trafficking pathways in a pH dependent manner.

Figure 1. Crystal structure of the KDEL receptor. **A.** Representative curves showing normalised binding of [³H]-TAEKDEL peptide to the KDEL receptor at different pH conditions. **B.** Crystal structure of KDELR viewed from the Golgi membrane. The transmembrane helices are labelled by number. Inset, topology of the fold, highlighting the two triple helix bundles (THB1 & THB2). **C.** Electrostatic surface representation of KDELR highlighting the negatively charged band on the cytosolic side of the receptor. **D.** View rotated 90° showing placement of the receptor with respect to the membrane bilayer (dashed lines). **E.** Sliced through volume representation of D. highlighting the polar cavity on the luminal side of the receptor.

Figure 2. Molecular basis for KDEL peptide recognition. **A.** The polar cavity in KDELR is shown with contributing side chains represented as sticks and their electrostatic surface shown. The bound TAEKDEL peptide is shown with the *mFo-DFc* difference electron density (green mesh) used for model building displayed, contoured at 3σ. The N-terminal threonine was disordered in the maps and not modelled. Waters are represented as spheres (red) with hydrogen bonds as dashed lines (yellow). **B.** Close up view of the polar cavity showing the structural movement induced in TM1 and TM6 upon peptide binding. The apo structure is shown in colored helices, peptide bound structure in grey. In the top down view (right), only the C-terminal leucine of the peptide is shown. **C.** Close up view of the polar cavity shown in panel A. Waters are represented as spheres (red) with hydrogen bonds as dashed lines (yellow). **D.** Overlay of the apo (colour-coded helices) and peptide-bound structure (grey) highlighting the short hydrogen bond formed between Glu127 and Tyr158 at the base of the polar cavity

following peptide binding. Two water molecules coordinate the interaction between the C-terminus of the peptide with Tyr158 and His12.

Figure 3. Functional characterisation of binding site mutations. **A.** *In vitro* binding assay using purified chicken KDEL receptor. (* indicates protein that was unable to be produced). **B.** ER retrieval assays were performed in the absence (-) or presence (+) of KDEL^{Sec} and the Golgi signal for KDEL receptor is plotted as mean \pm SEM. **C.** KDEL receptors were tested for KDEL^{Sec}-induced redistribution from Golgi to ER as in **B**. TGN46 was used as a Golgi marker. Scale bar is 10 μ m.

Figure 4. Structural basis for exposure of COPI retrieval signal. **A.** Overlay of the apo (grey) and peptide-bound (colored helices) crystal structures of the KDEL_R. The movement of TM7 is highlighted, exposing the C-terminal lysine side chains, indicated by the dashed circle. Right, cytoplasmic view of the receptor with the movement in TM7 indicated. **B.** Electrostatic surface representation of panel A. Dashed lines indicate rough position of the Golgi membrane, and the lysine retrieval motif is indicated by the dashed circle. Following movement of TM7, a new cavity opens on the cytoplasmic side of the receptor, exposing Asp193. **C.** Cytoplasmic surface of the receptor, showing the substantial change in distribution of surface charge, most notably the disruption of the negative band present in the apo state. **D.** Wild-type, Asp193Asn and KGKK-dilysine motif mutant KDEL receptors were tested for KDEL^{Sec}-induced redistribution from Golgi to ER. TGN46 was used as a Golgi marker. Scale bar is 10 μ m. **E.** Golgi signal for KDEL receptor in retrieval assays performed as in panel D in the absence (-) or presence (+) of KDEL^{Sec} is plotted as mean \pm SEM.

Acknowledgements: We thank the staff of beamlines I24 Diamond Light Source, UK for assistance. **Funding:** This work was supported by Wellcome awards (102890/Z/13/Z, 109133/Z/15/A & 097769/Z/11/Z) to SN and FAB and SNSF Professorship of the Swiss National Science Foundation (PP00P3_144823) & Commission for Technology and Innovation CTI (16003.1 PFLS-LS) to MAS. **Author contributions:** SN, JLP, MAS & FB designed the experiments and interpreted the data. PB, JLP, AG, IZ & SN carried out the experiments and interpreted the data. PB, JLP, FB & SN wrote the paper. **Competing interests:** the authors declare no competing financial interests. **Data and materials**

availability: Atomic coordinates for the models have been deposited in the Protein Data Bank (PDB) under accession codes; 6I6J (Syb37-KDEL_{R2} complex), 6I6B (Apo structure) & 6I6H (peptide-bound structure).

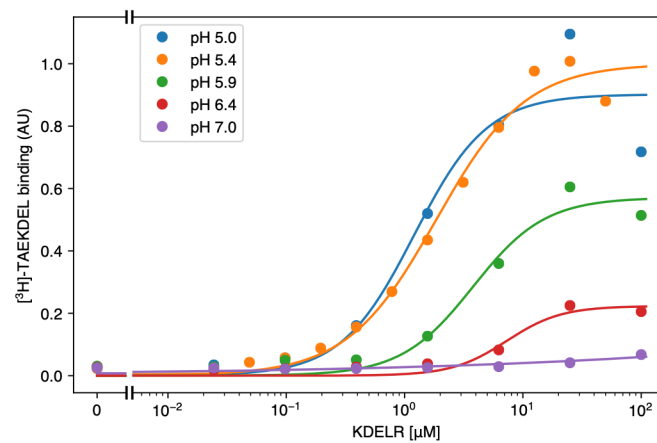
References

1. L. Ellgaard, A. Helenius, Quality control in the endoplasmic reticulum. *Nat Rev Mol Cell Biol* **4**, 181-191 (2003).
2. S. Munro, H. R. Pelham, A C-terminal signal prevents secretion of luminal ER proteins. *Cell* **48**, 899-907 (1987).
3. J. C. Semenza, K. G. Hardwick, N. Dean, H. R. Pelham, ERD2, a yeast gene required for the receptor-mediated retrieval of luminal ER proteins from the secretory pathway. *Cell* **61**, 1349-1357 (1990).
4. F. M. Townsley, G. Frigerio, H. R. Pelham, Retrieval of HDEL proteins is required for growth of yeast cells. *The Journal of cell biology* **127**, 21-28 (1994).
5. H. R. Pelham, K. G. Hardwick, M. J. Lewis, Sorting of soluble ER proteins in yeast. *The EMBO journal* **7**, 1757-1762 (1988).
6. L. Feng, W. B. Frommer, Evolution of Transporters: The Relationship of SWEETs, PQ-loop, and PnuC Transporters. *Trends Biochem Sci* **41**, 118-119 (2016).
7. M. J. Lewis, H. R. Pelham, Ligand-induced redistribution of a human KDEL receptor from the Golgi complex to the endoplasmic reticulum. *Cell* **68**, 353-364 (1992).
8. G. Griffiths *et al.*, Localization of the Lys, Asp, Glu, Leu tetrapeptide receptor to the Golgi complex and the intermediate compartment in mammalian cells. *The Journal of cell biology* **127**, 1557-1574 (1994).
9. D. W. Wilson, M. J. Lewis, H. R. Pelham, pH-dependent binding of KDEL to its receptor in vitro. *The Journal of biological chemistry* **268**, 7465-7468 (1993).
10. M. M. Wu *et al.*, Organelle pH studies using targeted avidin and fluorescein-biotin. *Chem Biol* **7**, 197-209 (2000).
11. M. M. Wu *et al.*, Mechanisms of pH regulation in the regulated secretory pathway. *The Journal of biological chemistry* **276**, 33027-33035 (2001).
12. I. Majoul, M. Straub, S. W. Hell, R. Duden, H. D. Soling, KDEL-cargo regulates interactions between proteins involved in COPI vesicle traffic: measurements in living cells using FRET. *Developmental cell* **1**, 139-153 (2001).
13. S. R. Pfeffer, Unsolved mysteries in membrane traffic. *Annual review of biochemistry* **76**, 629-645 (2007).

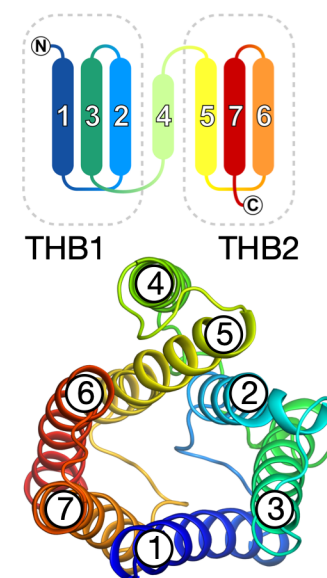
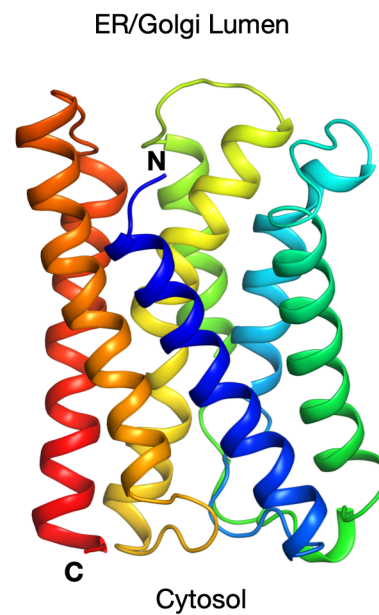
14. N. Gomez-Navarro, E. Miller, Protein sorting at the ER-Golgi interface. *The Journal of cell biology* **215**, 769-778 (2016).
15. Y. Tao *et al.*, Structure of a eukaryotic SWEET transporter in a homotrimeric complex. *Nature* **527**, 259-263 (2015).
16. F. M. Townsley, D. W. Wilson, H. R. Pelham, Mutational analysis of the human KDEL receptor: distinct structural requirements for Golgi retention, ligand binding and retrograde transport. *The EMBO journal* **12**, 2821-2829 (1993).
17. C. Barlowe, Signals for COPII-dependent export from the ER: what's the ticket out? *Trends Cell Biol* **13**, 295-300 (2003).
18. H. J. Sharpe, T. J. Stevens, S. Munro, A comprehensive comparison of transmembrane domains reveals organelle-specific properties. *Cell* **142**, 158-169 (2010).
19. J. L. Parker, S. Newstead, Structural basis of nucleotide sugar transport across the Golgi membrane. *Nature* **551**, 521-524 (2017).
20. A. A. Scheel, H. R. Pelham, Identification of amino acids in the binding pocket of the human KDEL receptor. *The Journal of biological chemistry* **273**, 2467-2472 (1998).
21. F. Letourneur *et al.*, Coatamer is essential for retrieval of dilysine-tagged proteins to the endoplasmic reticulum. *Cell* **79**, 1199-1207 (1994).
22. L. P. Jackson *et al.*, Molecular basis for recognition of dilysine trafficking motifs by COPI. *Developmental cell* **23**, 1255-1262 (2012).
23. I. Zimmermann *et al.*, Synthetic single domain antibodies for the conformational trapping of membrane proteins. *eLife* **7**, (2018).

Figure 1

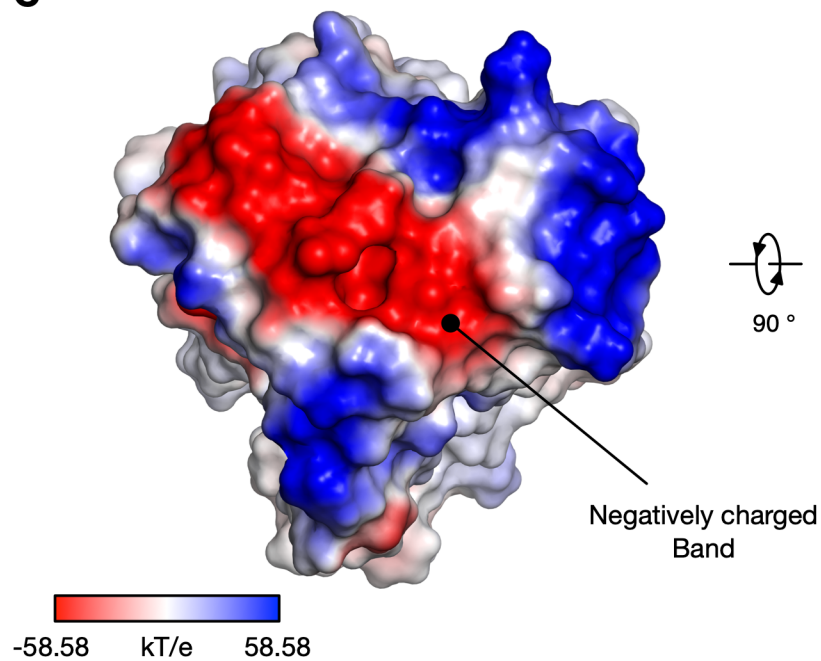
A



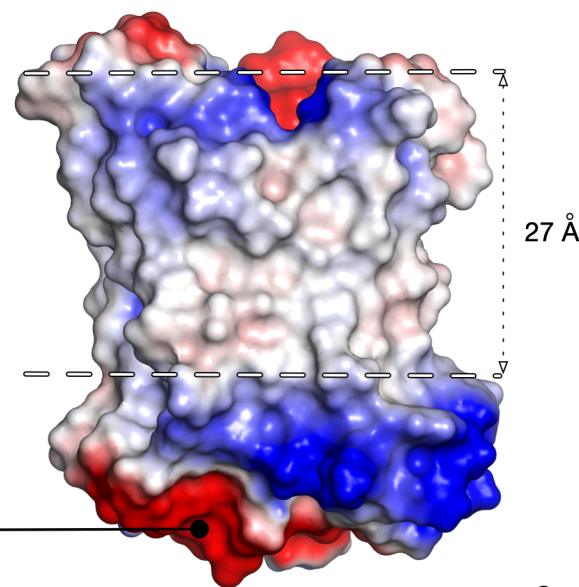
B



C



D



E

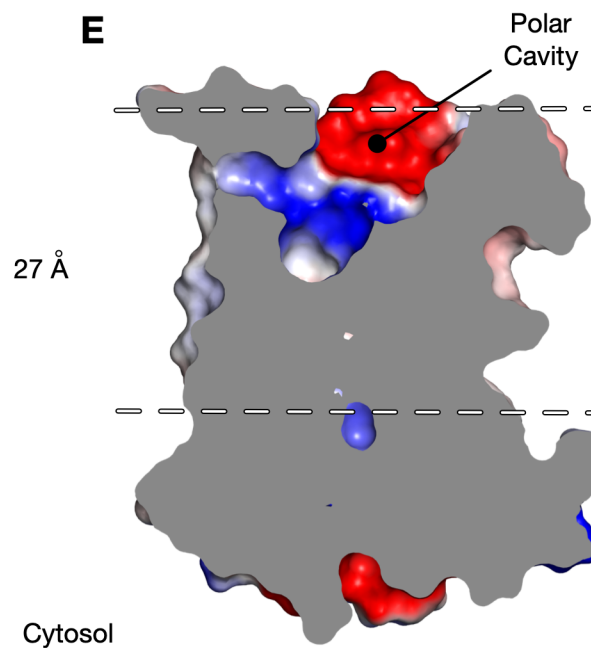


Figure 2

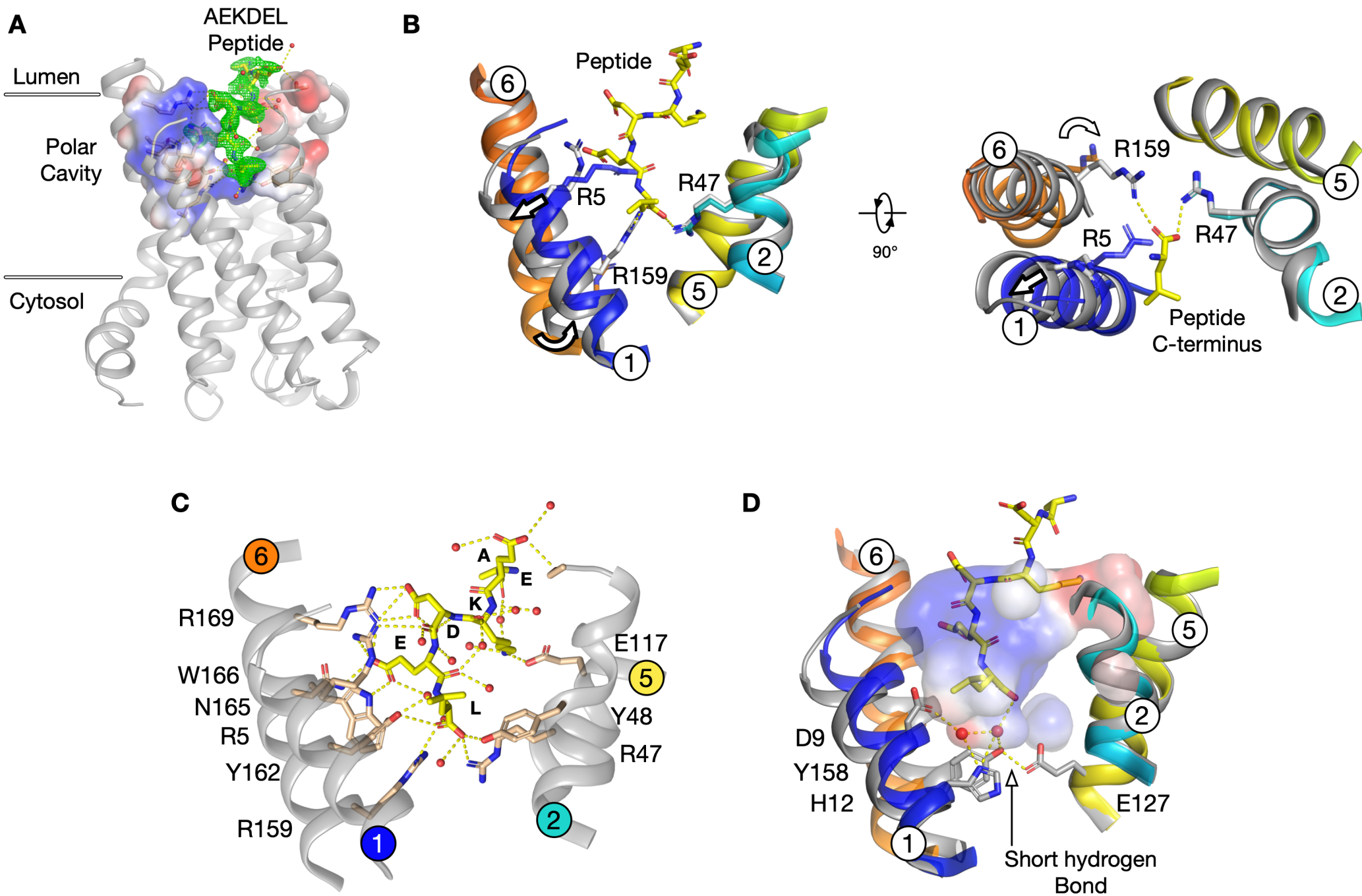


Figure 3

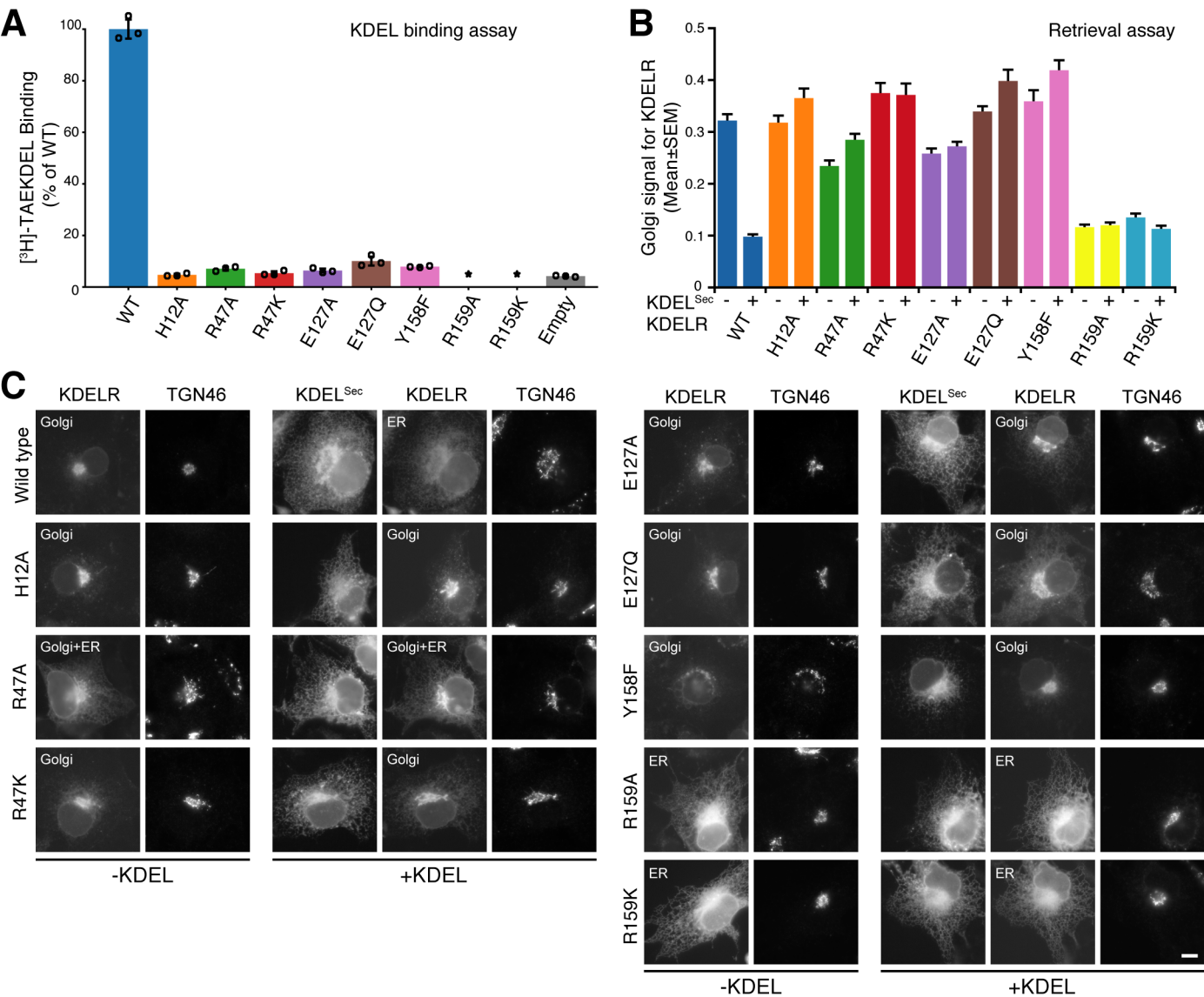
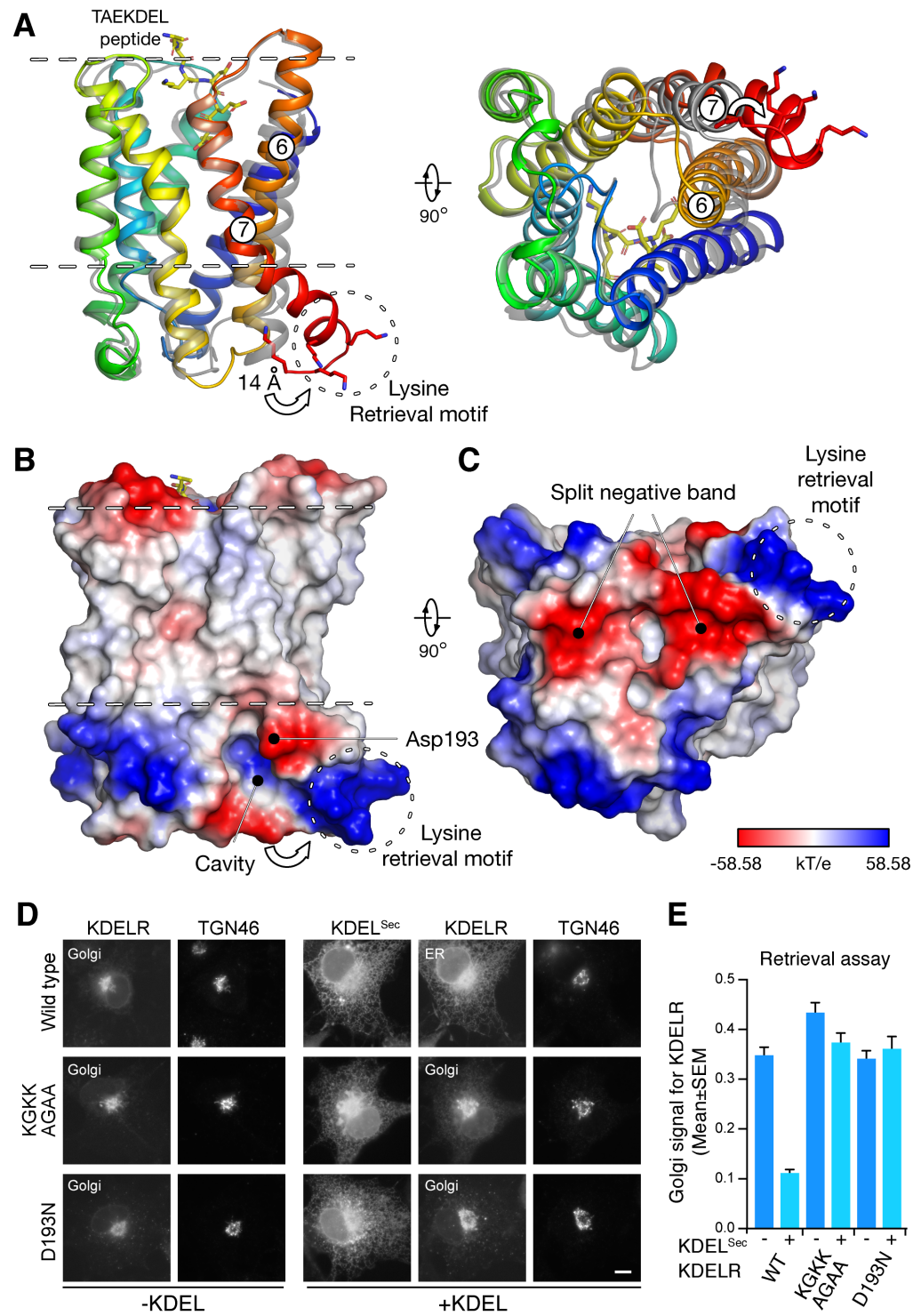


Figure 4





Supplementary Materials for

Structural basis for pH-dependent retrieval of ER proteins from the Golgi by the KDEL receptor.

Philipp Bräuer¹, Joanne L. Parker¹, Andreas Gerondopoulos¹, Iwan Zimmermann²,
Markus A. Seeger², Francis A. Barr^{1*}, & Simon Newstead^{1*}.

Correspondence to: simon.newstead@bioch.ox.ac.uk & francis.barr@bioch.ox.ac.uk

This PDF file includes:

Materials and Methods
Supplementary Text
Figs. S1 to S13
Table S1
Supplementary references

Materials and Methods

Cloning, expression and purification of KDELR

The genes encoding for *Gallus gallus* (Gg) KDELR2 (Uniprot: Q5ZKX9) and *Mus musculus* (Mm) KDELR1 (Uniprot: Q99JH8) were codon optimised and cloned into a modified form of a C-terminal GFP^{His} fusion vector for expression *Saccharomyces cerevisiae* strain BY5460 (24). Specifically, Wild-type and mutant forms of the KDELR gene were expressed by growing an overnight culture in synthetic complete medium minus leucine with 2% glucose (w/v). This culture was diluted tenfold in medium minus leucine with 2% lactate (v/v) in a 15 L fermentation vessel (Eppendorf BioFlo 415, DE); variants, as detailed in the text, were grown in flasks in 0.8 L of media. After 24 h, expression was induced through the addition of 1.5% galactose (w/v). After a further 24 h the yeast were collected and membranes prepared as described in (25). Wild type KDELR2 and variants were purified to homogeneity (Fig. S12), using standard immobilised metal-affinity chromatography (IMAC) in n-dodecyl- β -D-maltopyranoside (Glycon, DE) (DDM) with cholesteryl hemisuccinate (Sigma, UK) (DDM-CHS) detergent, as described previously (26). Briefly, membrane fractions were solubilised in 20 mM Tris pH 7.50, 0.1M NaCl, 1% DDM, 0.5% CHS for two hours. The soluble fraction was then bound to Ni-NTA resin (Pierce/Thermo, USA) in 20 mM Tris pH 7.50, 0.1M NaCl, 0.1% DDM, 0.05% CHS and subsequently eluted with 250 mM imidazole. After overnight dialysis with Tobacco Etch Virus (TEV) protease in 20 mM Tris pH 7.50, 0.15 M NaCl, 0.03% DDM, 0.0015% CHS, a reverse IMAC purification step was performed. The flow through was concentrated in a 10 kDa molecular weight cut off (MWCO) spin concentrator (VivaSpin, Sartorius) and applied to a Superdex 200 (10/300) column (GE Healthcare) in 20 mM Tris pH 7.50, 0.1M NaCl, 0.03% DDM, 0.0015% CHS.

Sybody selection and purification

Sybody selection was performed against C-terminally Avi-tagged and biotinylated Mm KDELR1, prepared using the same procedure as for Gg KDELR2. The protocols for sybody selection have been described elsewhere (27). A high affinity sybody (K_D 14.8 nM \pm 1.7), Syb37, was identified from the loop library (27), which formed a stable complex with the receptor and co-eluted down a SRT-C SEC 300 column (Sepax, USA). Biolayer interferometry was performed on an Octet Red 384 (PALL, USA) using streptavidin biosensors which were loaded with biotinylated Gg KDELR2 at 0.1 mg mL⁻¹ (Fig. S13). K_D measurements were performed using a serial dilution of the sybody from 500 nM to 7.8 nM. A 60 s baseline step

in 20 mM Tris-HCl, 150 mM NaCl, 0.03% DDM, 0.0015% CHS was followed by a 300 s association step in the desired sybody concentration, followed by a 300 s dissociation step. Data were analysed in the Octet v9.0 software package. All raw data was baseline and reference subtracted, in-step corrected, y-axis aligned and filtered with a Savitzky-Golay filter.

Crystallisation and structure determination

Peptide-free Apo structure: The protein-laden mesophase was prepared by homogenizing monoolein (Sigma, UK) and 15.5 mg.mL⁻¹ Gg KDELR2 in a 60:40 ratio by weight using a dual-syringe mixing device at 20 °C (28). Crystallisation was carried out at 19 °C using the Gryphon LCP robot in a 96 well glass sandwich plate (Thermo, USA) using 50 nL mesophase and 0.8 µL precipitant solution, consisting of 30% (v/v) PEG 500 DME, 100 mM Tris pH 9.0 and 100 mM Magnesium sulphate. Crystals were grown at 4 °C and harvested 10 days after setting up using a tungsten carbide glasscutter to open the plates and employing 30 – 75 µm micromounts (MiTeGen, USA) to harvest the crystals, which were subsequently cryocooled in liquid nitrogen and stored prior to data collection. Data from apo crystals were collected at the microfocus beamline I24 (Diamond Light Source, UK). All data were processed and scaled using the Xia2 (29) pipeline to DIALS (30) and AIMLESS (31) (Supplementary Table 1). No crystals were obtained for the apo receptor in acidic pH conditions. **Peptide bound structure:** Gg KDELR2 was concentrated to 14.5 mg mL⁻¹ and incubated with 6.4 mM TAEKDEL peptide (Cambridge Peptides, UK) on ice for one hour prior to crystallisation. Crystallisation plates were set up and left at 19 °C using precipitant 30% (v/v) PEG 600, 100 mM MES pH 6.0, 100 mM Sodium Nitrate. **Sybody-complex structure:** Gg KDELR2 Syb37 complex was concentrated to ~ 15 mg mL⁻¹ after being bound on ice for 1 h and subsequently applied to an SRT-C SEC 300 SEC column (Sepax, USA). Fractions containing the complex were pooled and concentrated to 15.4 mg mL⁻¹. Crystallisation plates were set up at 19 °C as above, with crystals forming after 2 days in 30% (v/v) PEG 400, 100 mM Tris pH 9.0.

Phases were initially determined from the Gg KDELR2-Syb37 complex via molecular replacement using Phaser (32), employing PDB:5M13 as the search model. The initial phases produced a map that contained interpretable density for the receptor and a model was subsequently built into the density using O (33) and Coot (34), followed by refinement in Phenix (35) and BUSTER (36). The peptide-free and bound structures were phased using molecular replacement employing the KDELR model built into maps calculated from the

Syb37 complex crystals. The distance of the short hydrogen bond in the peptide bound complex (PDB: 6I6H) was fixed at 2.5 Å using the LINK command in BUSTER. However, refinement in Phenix suggested a shorter distance of ~ 2.3 Å.

Peptide binding assays

Binding assays were performed in 20 mM MES pH 5.4, 40 mM Sodium Chloride, 0.01% DDM 0.0005% CHS unless stated otherwise. 5 µL of ³H-TAEKDEL (Cambridge Research Biochemicals, UK) at 20 nM was incubated with 5 µL of Gg KDEL_R, purified as above, or variants thereof at the desired concentration, at 20 °C for 10 min. The reaction was then filtered through a 0.22 µm mixed cellulose ester filters (Millipore, USA) using a vacuum manifold. Filters were then washed with 2 x 500 µL cold buffer. The amount of peptide remaining bound was measured using scintillation counting in Ultima Gold (Perkin Elmer). Experiments were performed at least three times, independently, to generate an overall mean and standard deviation (s.d). Data were normalised to the maximal binding at pH 5.4 and fit with a three-parameter non-linear regression model.

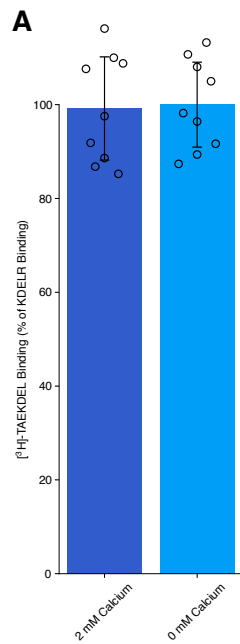
ER retrieval assays

Homo sapiens KDEL_R1 (Uniprot: P24390) was cloned into a pEF5/TO/FRT vector with a C-terminal 20 amino acid linker made up of 5 copies of Gly-Ser-Ser-Ser followed by GFP to create KDEL_R-GFP. Specific point mutations, described in the figures, were introduced using the Quickchange protocol (Stratagene, USA). To create the cytoplasmic targeted sybody (Syb37^{Cyto}) human codon optimised Syb37 produced using gene synthesis was cloned into a pcDNA3.1+ vector with the same C-terminal linker followed by mScarlet. The secretory pathway targeted Sybody37 construct (Syb37^{Sec}) was created by addition of amino acids 1-26 of human growth hormone (hGH) (the signal peptide) in-frame and upstream of the sybody start codon. To create the mScarlet-KDEL ligand construct, mScarlet with the N-terminal hGH signal peptide and the 16 C-terminal residues of human BiP at its C-terminus, containing the KDEL signal, was cloned into the pcDNA4 vector. COS7 cells were grown on 10 mm diameter 0.16-0.19 mm thick glass coverslips in DMEM containing 10% (v/v) bovine calf serum at 37°C and 5% CO₂. Cells were plated at 50,000 cells per well of a 6-well plate, each well containing 2 coverslips. For ER retrieval assays, the cells were transfected after 18h with 0.5 µg pEF5/TO/FRT KDEL_R-GFP and 0.5 µg pcDNA4 mScarlet-KDEL ligand (+ligand) or 0.5 µg pEF5/TO/FRT KDEL_R-GFP and 0.5 µg pcDNA4 empty vector (-ligand) diluted in 100µl

Optimem and 3 μ l Mirus LT1 (Mirus Bio LLC). For Golgi localisation assays using Syb37, the cells were transfected after 18h with 0.5 μ g pEF5/TO/FRT KDELR-GFP and 0.5 μ g pcDNA3.1+ Syb37^{Sec} or 0.5 μ g pEF5/TO/FRT KDELR-GFP and 0.5 μ g pcDNA3.1+ Syb37^{Cyto}. After a further 22 h, cells were washed twice with 2 mL of PBS, then fixed for 2 h in 2 mL PLP (2% w/v) paraformaldehyde in 87.5 mM lysine, 87.5 mM sodium phosphate pH 7.4, and 10 mM sodium periodate). Subsequently, coverslips were washed three times in 2 mL permeabilization solution 100 mM sodium phosphate pH 7.4, then permeabilised in 1 mg mL⁻¹ BSA, 0.12 mg mL⁻¹ saponin, and 100 mM sodium phosphate pH 7.4 for 30 min. Primary and secondary antibody staining was performed for 60 min in permeabilization solution at 22°C. Commercially available antibodies were used to detect TGN46 (sheep; AbD Serotec) and LAMP1 (mouse clone H4A3; BD). Coverslips were mounted on glass slides in Mowiol 4-88 and imaged with a 60 \times /1.35 NA oil immersion objective on an Olympus BX61 upright microscope (with filtersets for DAPI, GFP/Alexa-488, -555, -568, and -647 (Chroma Technology Corp.), a 2048x2048 pixel CMOS camera (Prim Σ ; Photometrics), and MetaMorph 7.5 imaging software (Molecular Dynamics Inc.). Illumination was provided by a wLS LED illumination unit (QImaging). Image stacks of 3-5 planes with 0.3 μ m spacing through the ER and Golgi were taken. The image stacks were then maximum intensity projected and the selected channels merged to create 24-bit RGB TIFF files in MetaMorph.

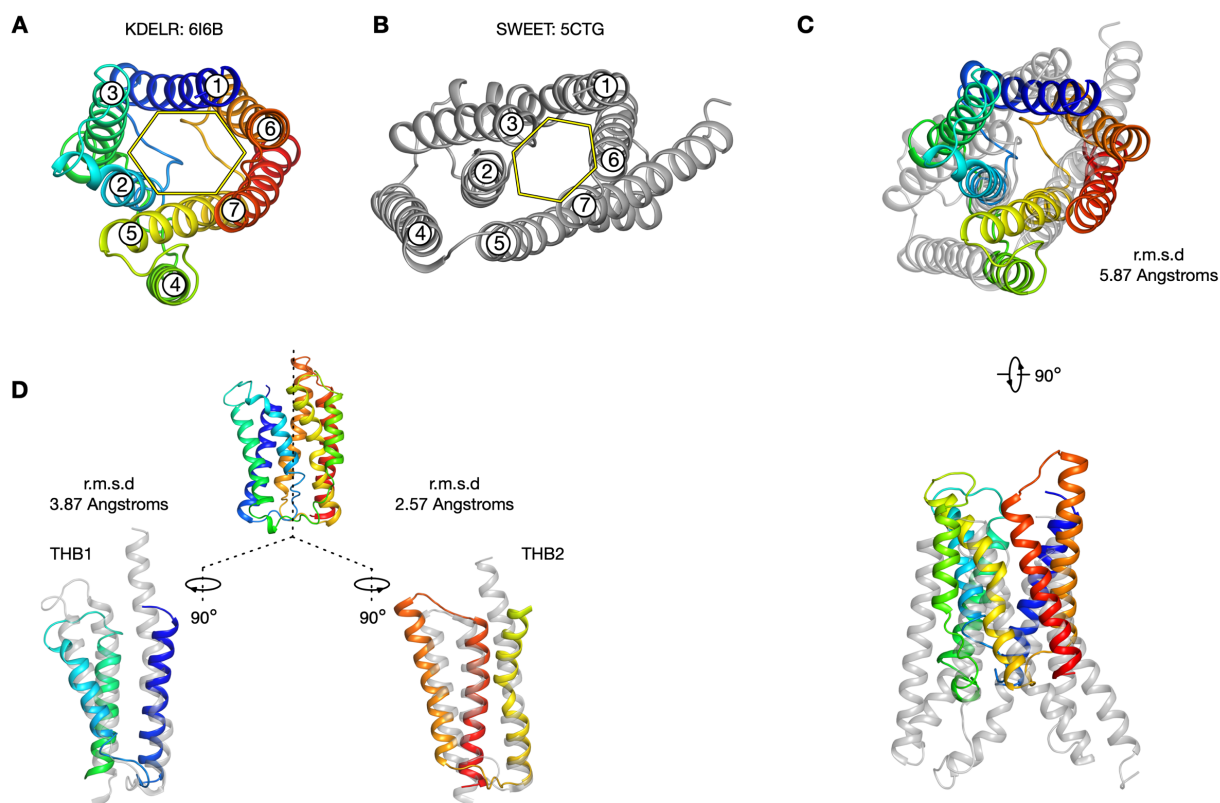
To produce the figures, images in 24-bit RGB format were cropped in Photoshop to show individual cells and then placed into Illustrator (Adobe Systems Inc., USA). To determine ER retrieval efficiency, the Golgi signal (integrated pixel intensity) for the KDELR receptor was measured in the region defined by the Golgi marker antibody in the presence (+) and absence (-) of KDEL ligand (37). Total cell KDELR signal (integrated pixel intensity) was also measured. For each cell, Golgi KDELR signal was divided by the total KDELR signal, to account for different expression levels, then plotted as a fraction in bar graph format. Error bars indicate the SEM. In Figure 3B n for WT=28, H12A=23, R47A=23, R47K=30, E127A=39, Y158F=22, R159A=23 and R159K=22. For Figure 4E n for WT=27, KGKK mutant=27 and D193N=44. Line intensity measurements of the different channels were used to examine the effect of Syb37 on KDELR localisation. These were plotted in line graphs.

Fig. S1.



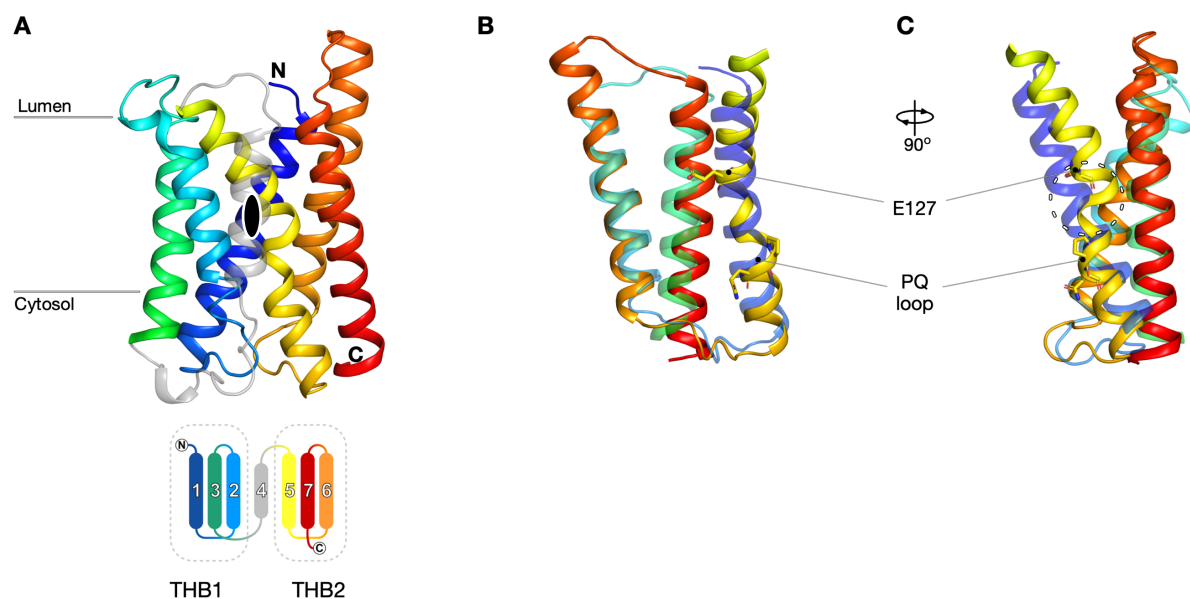
Peptide binding to the chicken KDEL receptor is independent of external calcium. A. Bar chart showing normalized binding of [³H]-TAEKDEL peptide to the *Gg*KDEL receptor in the presence (dark blue) and absence (light blue) of CaCl₂.

Fig. S2.



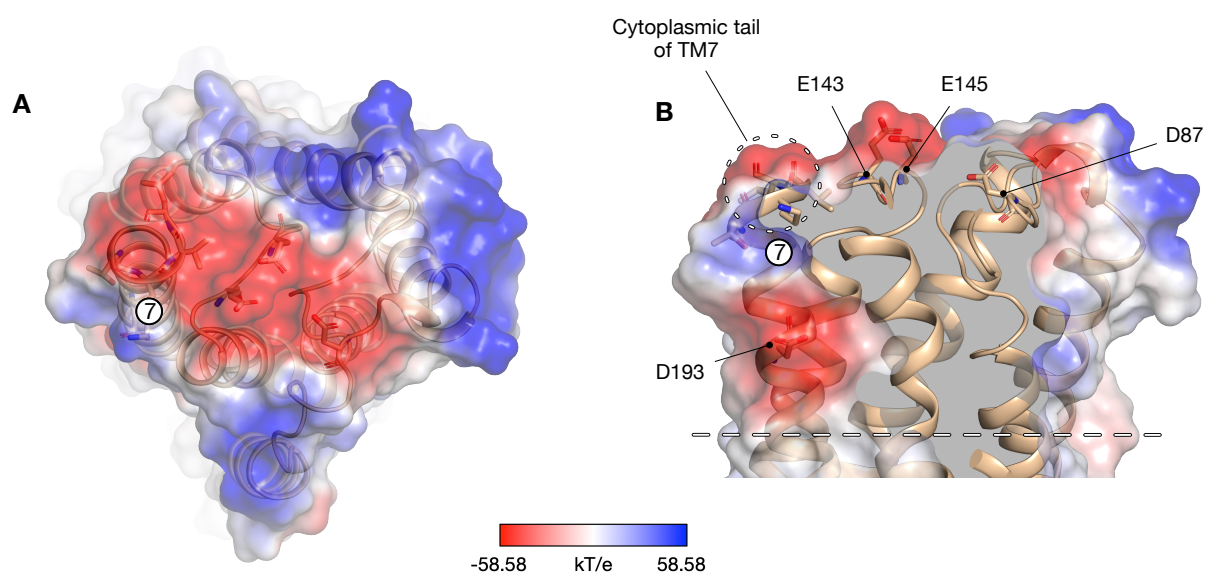
Structural comparison between the KDEL receptor and eukaryotic SWEET transporters. A. Luminal view of the KDEL receptor (PDB: 6I6B), coloured blue to red with TM helices labelled. The hexagonal arrangement of the TM helices is highlighted. **B.** Cytosolic view of the SWEET transporter from *O. sativa* (PDB: 5CTG), coloured grey, with TM helices labelled. A similar, though less obvious hexagonal arrangement of the helices can be discerned. **C.** Structural overlay of the KDEL receptor on the SWEET transporter using the cealign command in PyMOL. **D.** The KDEL receptor can be split into two triple helix bundles (THBs) as shown, which align better with the equivalent THBs in the SWEET transporter. Of particular note, TMs 1 and 5 are much shorter in the KDEL receptor relative to the vacuolar SWEET transporter (PDB:5CTG). TM4 was omitted for clarity.

Fig. S3.



Structural analysis of the KDEL receptor. **A.** View of KDEL receptor in the plane of the membrane, colored red to blue. TM4, which acts as linker between THB1 and THB2, has been greyed out for clarity. Below, topology diagram indicating the arrangement of the helices. The pseudo-two fold rotation axis that relates THB1 with THB2 is shown as a black oval. **B.** THB1 can be superimposed onto THB2 with an r.m.s.d of 2.54 Å over 72 Cα atoms. The residues that form the ‘PQ-loop’, for which the superfamily is named, are located on TM5 and shown as sticks. The PQ-loop motif occurs close to Glu127, which is important in forming the short hydrogen bond that clamps the KDEL peptide in the receptor. **C.** TM6 adopts an unusual kink (dashed circle), which facilitates the correct positioning of Glu127 in the receptor and might explain the requirement for the PQ motif.

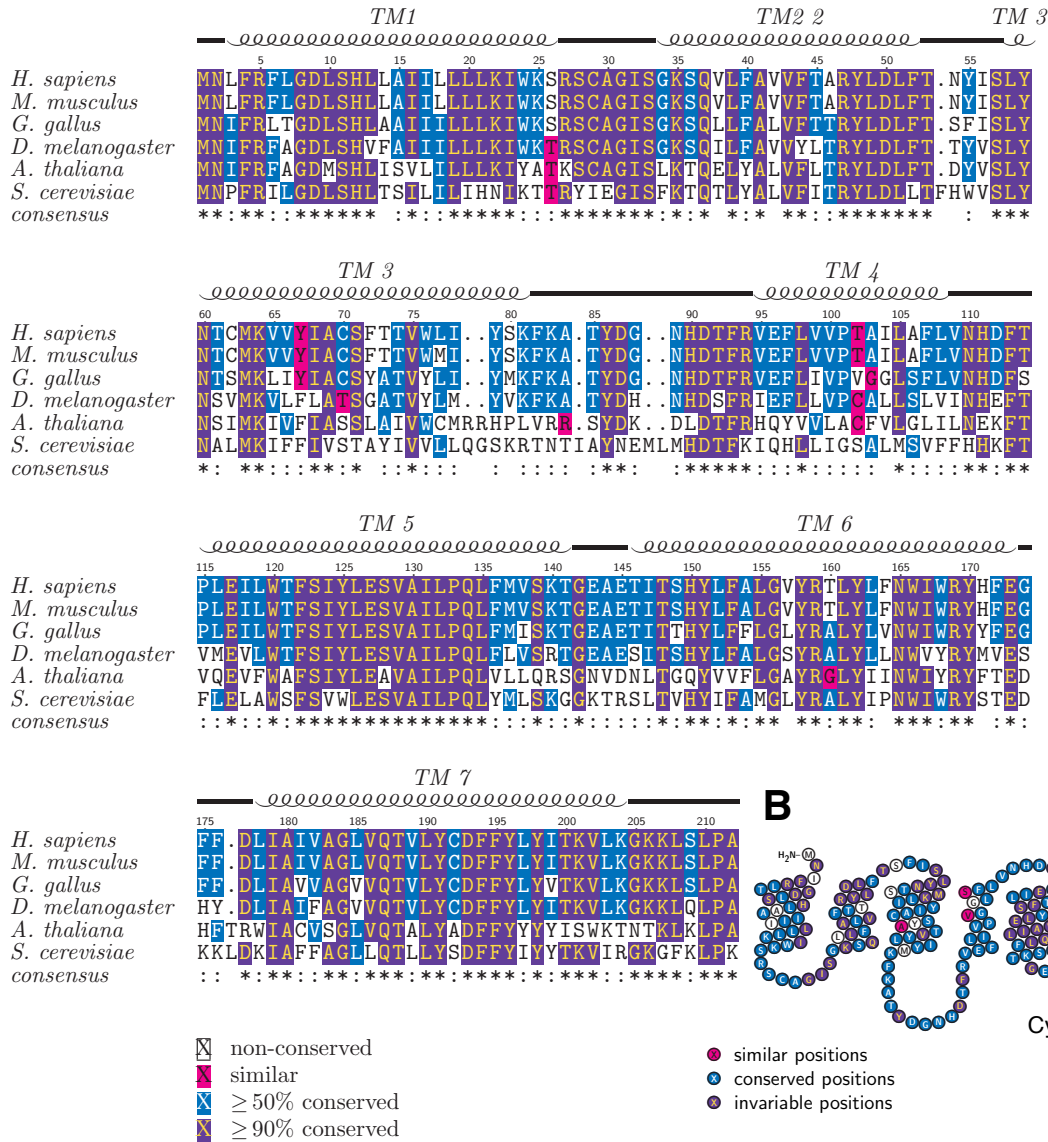
Fig. S4.



Analysis of the electrostatic surface charge on the KDEL receptor in the Apo state. **A.** Electrostatic surface of the cytosolic face of the KDEL receptor. Residues contributing to the prominent negatively charged patch are located on the loop regions connecting TM3 to TM4, and TM5 to TM6. The C-terminal end of TM7 also makes a considerable contribution to the negative charge, due to the free-carboxylic acid group and the carbonyl groups of the terminal residues. **B.** Sliced in view of the receptor in the membrane plane, cytosolic side facing up. Residues contributing to the negatively charged patch are labelled. D193 on TM7 is labelled, as this also contributes a distinctive negative charge close to the membrane surface (dashed line).

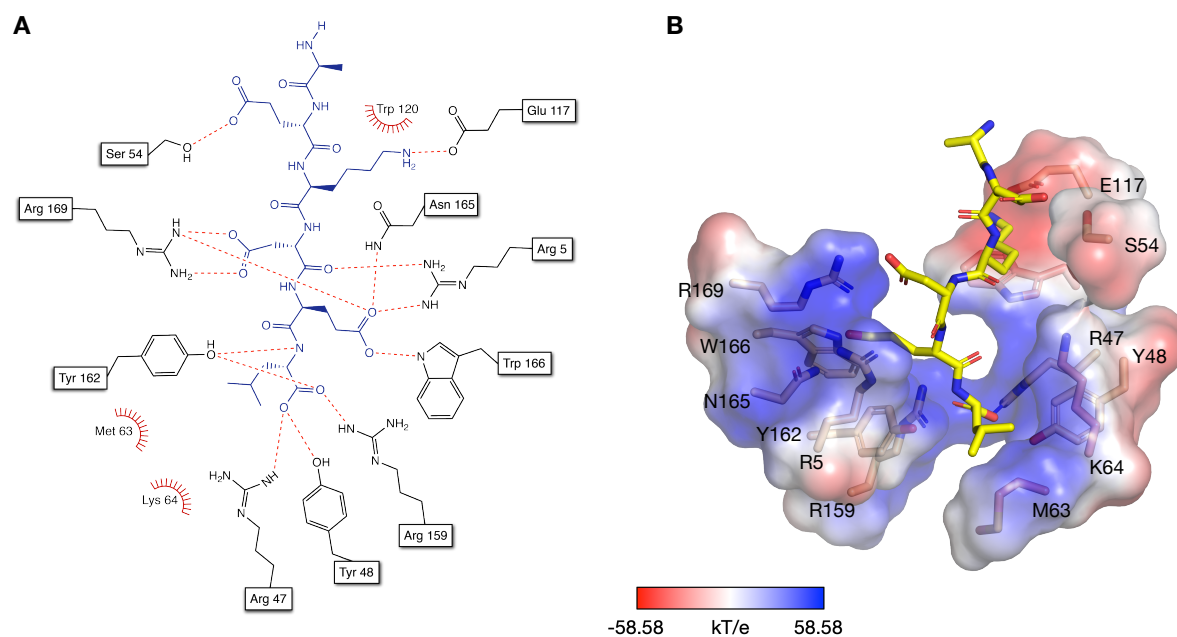
Fig. S5.

A



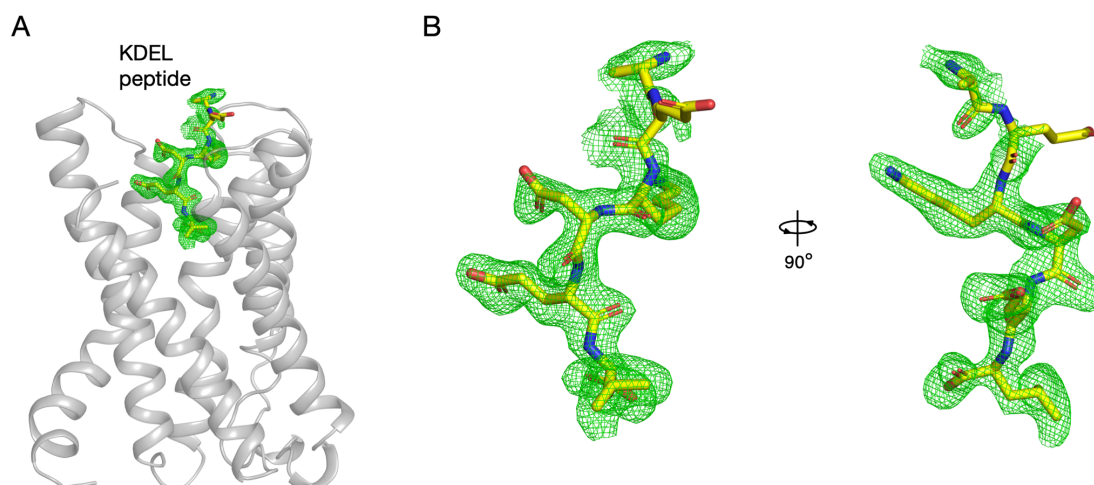
Sequence alignment and topology diagram of the KDEL receptor. **A.** Multiple sequence alignment between the KDEL receptors from *H. sapiens* (Uniprot: P24390), *M. musculus* (Q9CQM2), *G. gallus* (Q5ZKX9), *D. melanogaster* (O76767), *A. thaliana* (P35402), *S. cerevisiae* (P18414). **B.** Topology diagram drawn using the crystal structure, colored coded for sequence conservation.

Fig. S6.



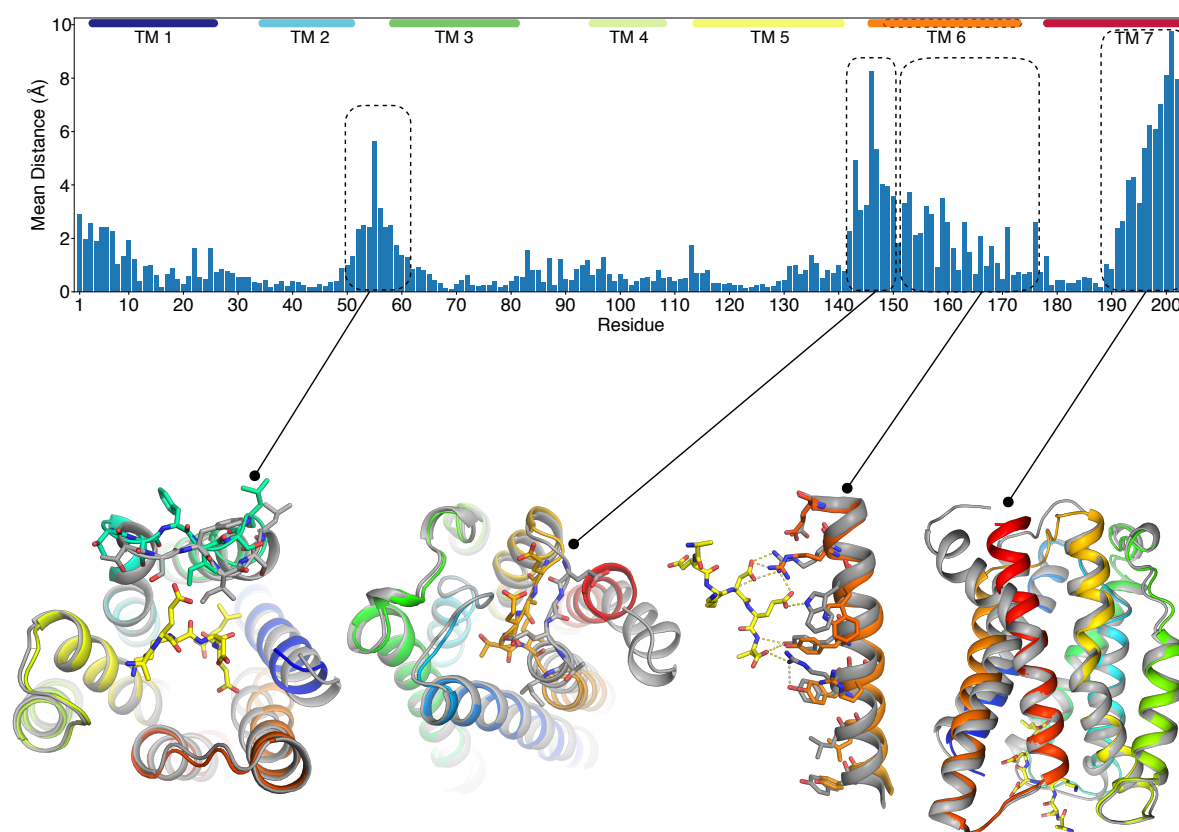
Molecular basis for KDEL peptide recognition. **A.** Schematic showing the interactions made between the KDEL peptide and receptor. Only the EKDEL region of the TAEKDEL peptide is shown as the two N-terminal residues do not interact with the receptor. Hydrogen bonds are shown as dashed lines (red), hydrophobic interactions as semi-circles (red). **B.** Electrostatic surface of the peptide binding cavity depicted.

Fig. S7.



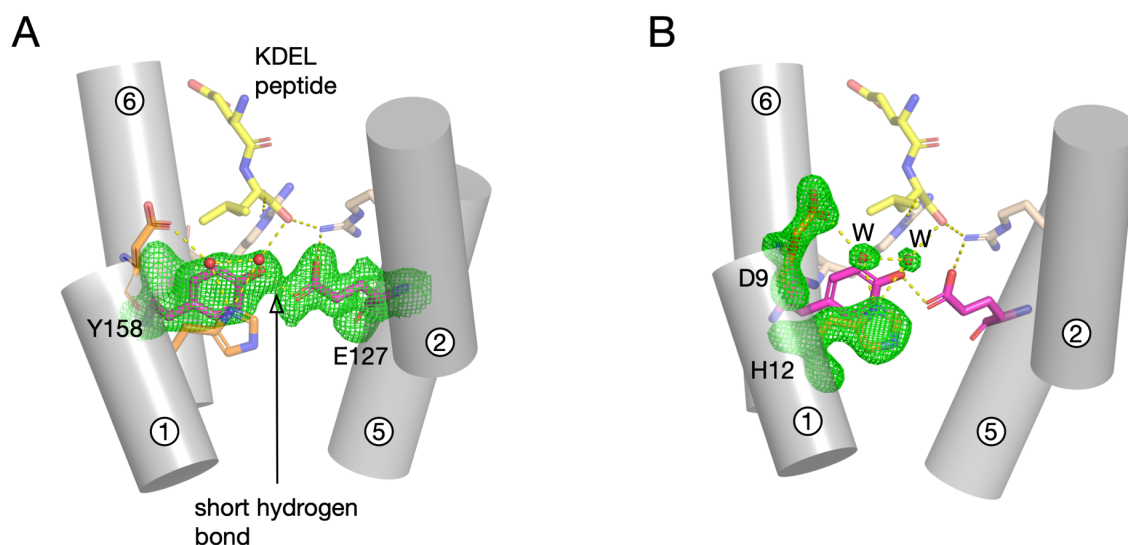
OMIT map showing the AEKDEL peptide captured in the receptor. A. Polder OMIT map (green mesh) contoured at 3σ , showing the position of the peptide in the KDELR, shown in cartoon (grey) in the plane of the membrane. **B.** Zoomed in view of the OMIT map shown in A. The density for the N-terminal threonine in the TAEKDEL ligand was too weak to model in the residue.

Fig. S8.



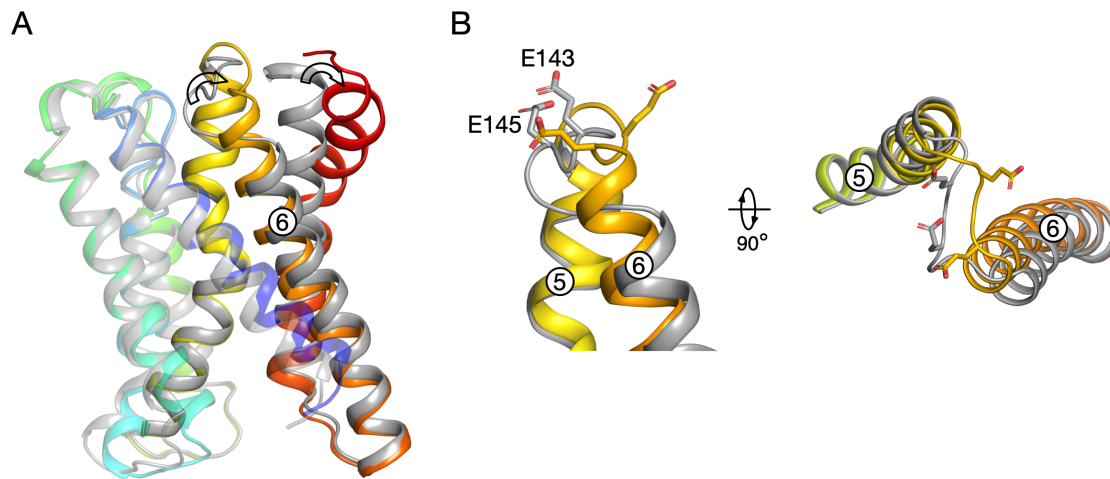
Comparison of receptor in peptide-bound and apo state. Plot showing the mean displacement of the center of each residue within the receptor upon peptide binding. The dashed boxes show regions of substantial movement and are highlighted on the structures below. The Apo structure is shown in Jones' rainbow (colored blue to red) representation while the peptide-bound structure is shown in grey. The TAEKDEL peptide is shown in yellow. The dashed red box around the TM6 label in the plot indicates the lesser extent of the helix in the Apo structure.

Fig. S9.



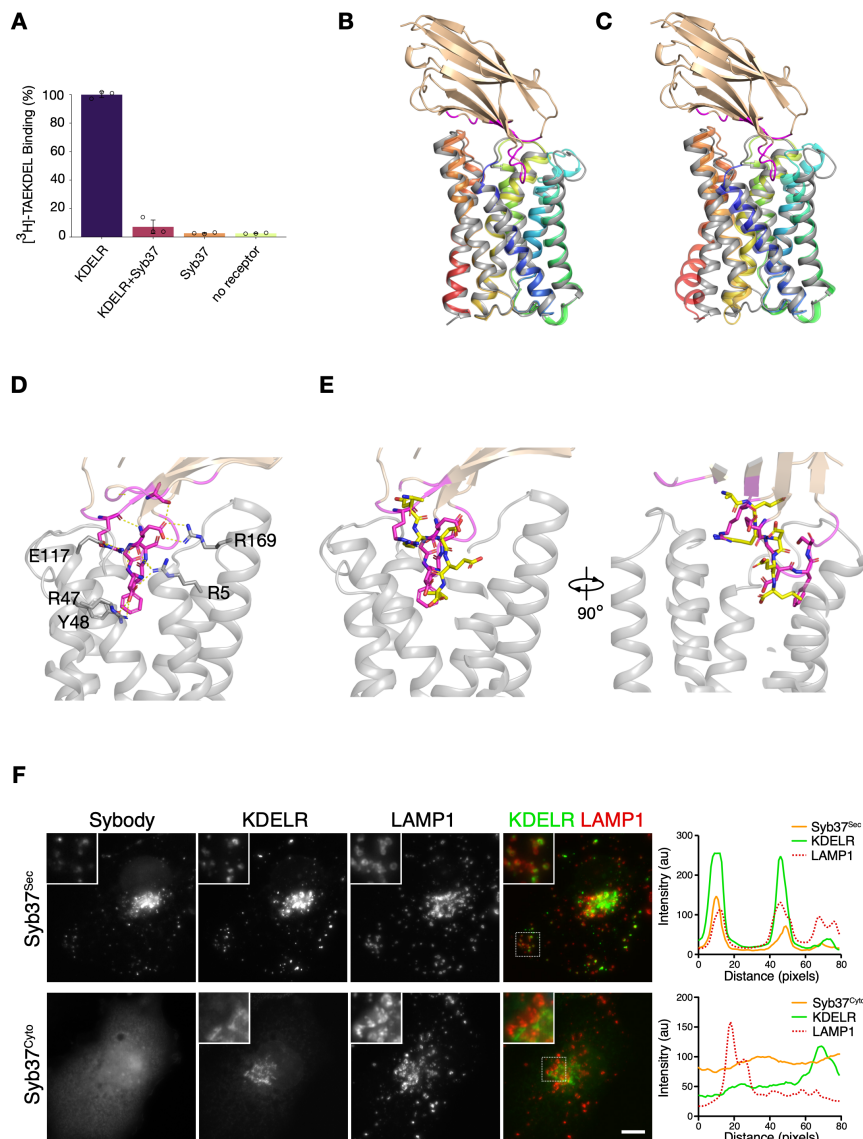
OMIT maps showing the short hydrogen bond interaction between Glu127 and Tyr158 upon peptide binding and water network. **A.** View of the short hydrogen bond formed between Glu127 and Tyr158 following binding of the TAEKDEL peptide (yellow sticks). The electron density from a Polder OMIT map is shown (green mesh), contoured at 3 σ , around Glu127 and Tyr158. Two water molecules are shown (red spheres), connecting Tyr158 to His12, suggesting a possible mechanism for pH sensing in the ER and Golgi. The second water molecule is observed forming a hydrogen bond to Asp9, mutation of which results in a receptor that is severely reduced in KDEL peptide binding (18). Hydrogen bonds shown as dashed lines (yellow). Arg47 and Arg159 (wheat sticks) are shown coordinating the carboxy terminus of the peptide. **B.** Equivalent view showing the Polder OMIT map (green mesh), contoured at 5 σ , around His12 and Asp9 and the two water molecules (W) linking these residues to Tyr158 and the carboxy terminus of the TAEKDEL peptide.

Fig. S10.



Structural comparison showing the movement of TM6 upon peptide binding. **A.** Overlay of the Apo (grey) and peptide-bound (colored blue to red) receptor structures with the movements in TM6 and TM7 indicated by arrows (open black). **B.** TM6 extends by one helical turn following the movement at the cytoplasmic end of TM7 upon peptide binding. This movement results in the repositioning of the conserved acidic side chains, Glu143 and Glu145, which contributes to the disruption of the negative electrostatic band projecting into the cytoplasm, and shown in Fig. S5.

Fig. S11.

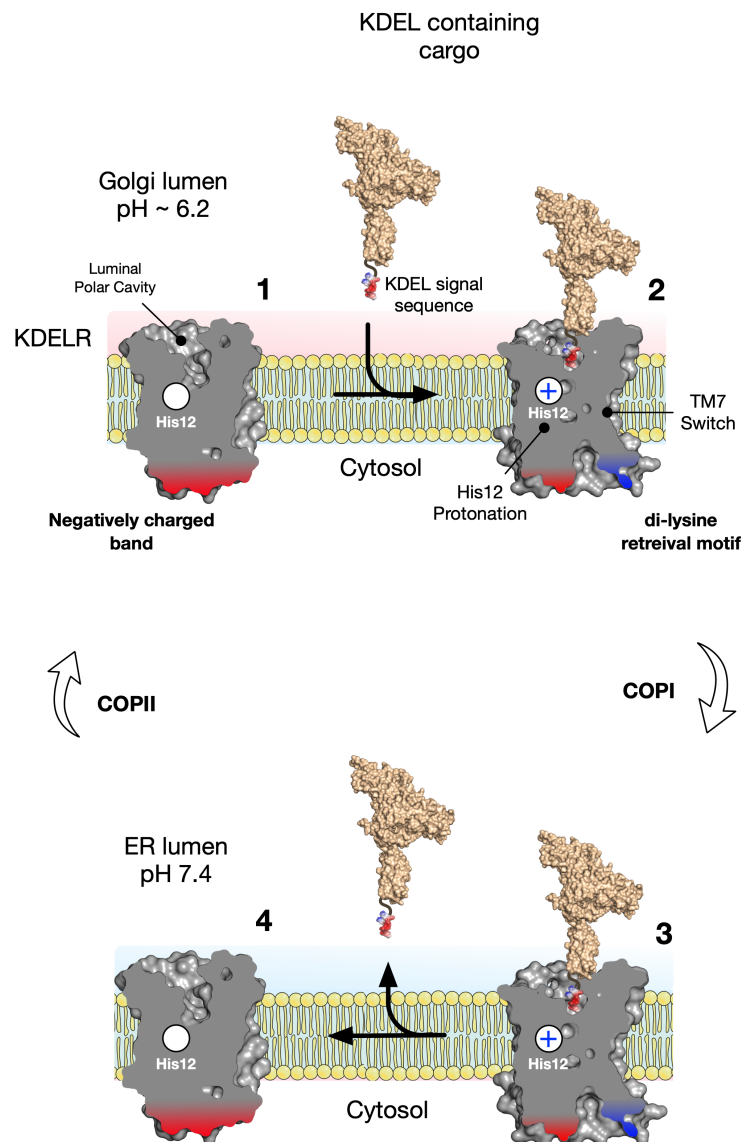


Syb37 block KDEL peptide binding but does not induce exposure of the di-lysine retrieval motif.

A. Bar chart showing binding of KDEL peptide to the receptor in detergent. **B.** Structural overlay of the KDELRL (grey) in complex with Syb37 (wheat) with the apo KDELRL structure (colored blue to red). The receptors overlay with an r.m.s.d. 0.73 Å. The variable regions of Syb37, including the CDR3 loop are shown in magenta. **C.** Equivalent overlay of the KDELRL-Syb37 complex on the peptide bound receptor, which overlays with an r.m.s.d. 1.97 Å. **D.** Zoomed in view of the polar cavity showing the interactions made to Syb37. Hydrogen bonds are shown as dashed lines. **E.** Superposition of the TAEKDEL peptide structure onto the KDELRL-Syb37 complex. The CDR3 loop (magenta sticks) occupies a similar position to the TAEKDEL peptide, but does not engage Arg159, instead interacting with Arg269 further along the helix. **F.** KDELRL localization in the presence of ER and Golgi luminal Syb37^{Sec} and cytoplasmic Syb37^{Cyto}. Cells were co-stained with the lysosomal marker LAMP1. Scale

bar is 10µm. Enlarged inset regions and line graphs show the co-localization of KDELR and Syb37^{Sec} to LAMP1-positive structures.

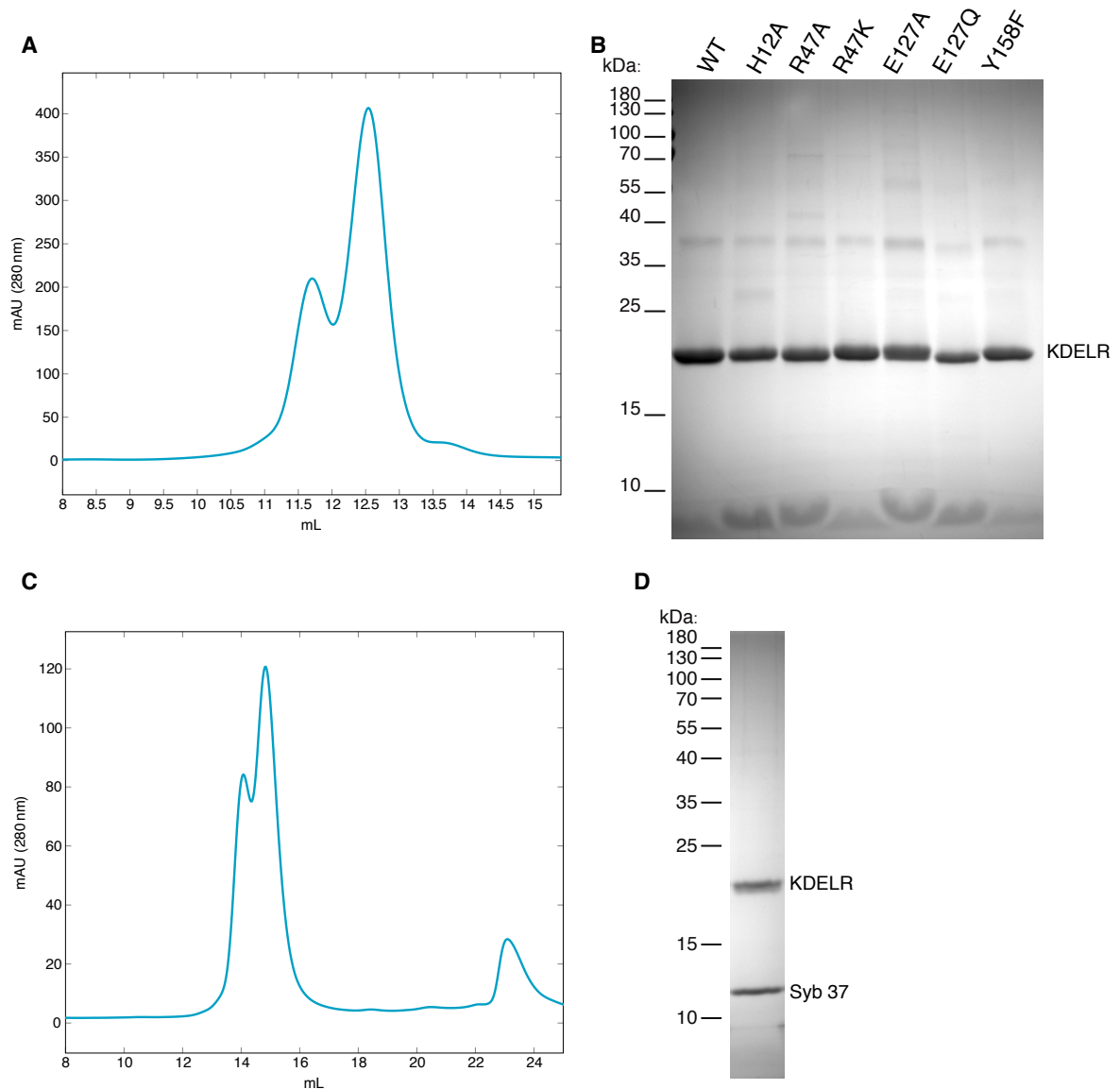
Fig. S11.



Model for pH-dependent retrieval of ER proteins from the Golgi by the KDEL receptor. Taken together, our data suggest a model for pH dependent retrieval of ER chaperones from the Golgi apparatus via the KDELR in mammalian cells. For Golgi to ER retrieval an empty receptor (**1**) must first bind to a KDEL protein in the luminal polar cavity at acidic pH (**2**). Binding results in the movement of TM1 and TM6, with the position of TM6 being stabilized through the formation of a strong hydrogen bond interaction between Tyr158 on TM6 and Glu127 on TM5, which serves to lock the peptide in place. Formation of this lock is likely facilitated through the protonation of His12 on TM1, acting as the pH sensor for the system. The movement of TM6 causes an outward rotation of the C-terminal end of TM7, resulting in substantial rearrangement of the electrostatic surface of the receptor facing the cytosol. The cytoplasmic negatively charged band present in the apo receptor (**1**) gives way to a more basic motif on TM7, as the C-terminal lysine side chains are exposed, revealing the likely

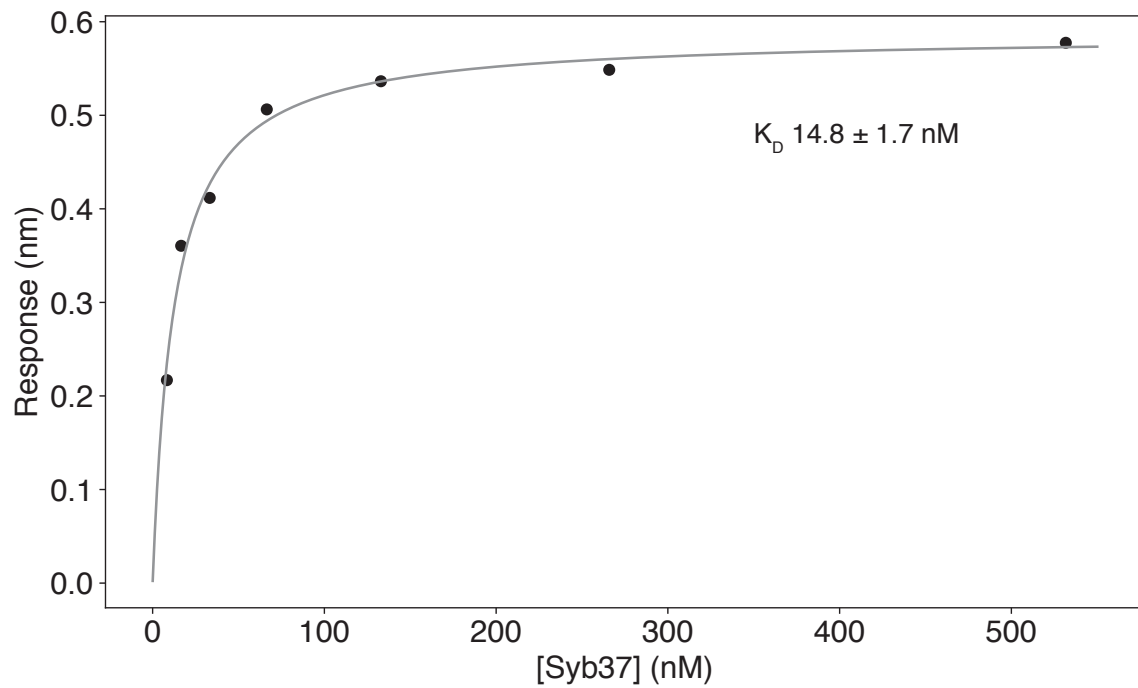
COPI binding site **(2)**. Following trafficking back to the ER, the change to neutral pH results in deprotonation of His12, causing TM1 and TM6 to move back and release the KDEL protein into the ER lumen **(3)**. As TM7 moves back, the C-terminal lysine motif packs against TM5, re-establishing the continuous negatively charged band, which may form part of a COPII binding motif **(4)**. The apo receptor is then trafficked back to the Golgi to repeat the cycle. The requirement for a pH modulated lock that requires the presence of the KDEL peptide to form, explains how this retrieval system is able to traffic ER chaperones against a millimolar concentration gradient using the extremely shallow pH gradient established between these two organelles. An important discovery from this work is that both the lysine COPI and putative acidic COPII recognition motifs are mutually exclusive, resulting in an elegant way for the KDEL receptor to switch between the ER to Golgi and Golgi to ER trafficking systems within the secretory pathway.

Fig. S12.



Purification of the KDEL R and the KDEL R-syb body complex. **A.** Size exclusion chromatography trace of the purified WT KDEL R on an S200 (10/300) Superdex column. The two peaks likely correspond to monomer and dimer of the KDEL receptor. **B.** SDS-PAGE analysis of the pooled peaked for the WT and variants of the receptor. **C.** Size exclusion chromatography trace of the WT KDEL R-Syb37 complex on an SRT-C SEC 300 SEC column. **D.** SDS-PAGE analysis of the SEC peak from **C.** showing formation of the complex.

Fig. S13.



Selection of a sybody with high affinity for the luminal face of the KDEL receptor. Representative curve for the binding of Syb37 to the GgKDEL_R using bilayer interferometry. The K_D was calculated from the mean of three independent experiments with the standard deviation shown.

Table S1. Crystallographic data table. Data collection and refinement statistics.

	KDEL _R (PDB: 6I6B)	KDEL _R + TAEKDEL (PDB: 6I6H)	KDEL _R -Syb37 (PDB: 6I6J)
Data Collection			
Space Group	C 2 2 2 ₁	P 2 ₁	P 2 ₁ 2 ₁ 2 ₁
Cell Dimensions			
<i>a</i> , <i>b</i> , <i>c</i> (Å)	47.90, 103.75, 101.59	47.87, 37.50, 62.75	50.40, 52.98, 133.06
α , β , γ (°)	90, 90, 90	90, 95.42, 90	90, 90, 90
Wavelength (Å)	0.969	0.969	0.969
Resolution (Å)	51.88-2.59 (2.66-2.59)	47.66-2.00 (2.05-2.00)	47.13 - 2.23 (2.29-2.23)
R _{pim}	0.158 (0.348)	0.096 (0.895)	0.055 (0.536)
R _{merge}	0.359 (1.069)	0.282 (2.588)	0.122 (1.247)
I/ σ I	4.1 (1.9)	6.8 (1.7)	7.0 (1.6)
Completeness (%)	99.9 (98.0)	99.2 (97.0)	99.5 (95.9)
Multiplicity	6.2 (6.3)	9.5 (9.1)	6.2 (6.3)
CC1/2	0.900 (0.519)	0.992 (0.721)	0.865 (0.536)
Wilson B-factor (Å ²)	23.7	22.6	40.9
Refinement			
No. reflections	50410	143906	111218
Unique Reflections	8183	15154	18108
R _{work} /R _{free}	0.24/0.27	0.19/0.23	0.21/0.25
No. atoms			
Protein	1680	1755	2638
(B _{res})*, protein atoms (Å ²)	30.8	25.5	49.1
(B _{res}), peptide atoms (Å ²)	n/a	36.4	n/a
(B _{res}), waters (Å ²)	27.7	44.3	48.4
(B _{res}), lipid atoms (Å ²)	51.0	65.5	67.9
Ramachandran favoured	97.0	97.6	97.5
Ramachandran outliers	0.0	0.0	0.0
R.M.S deviations			
Bond lengths (Å)	0.005	0.013	0.004
Bond angles (°)	0.96	1.49	0.95

* B_{res} are the residual B factors of the model.

References

24. J. L. Parker, S. Newstead, Method to increase the yield of eukaryotic membrane protein expression in *Saccharomyces cerevisiae* for structural and functional studies. *Protein Sci* **23**, 1309-1314 (2014).
25. J. L. Parker, S. Newstead, Structural basis of nucleotide sugar transport across the Golgi membrane. *Nature* **551**, 521-524 (2017).
26. D. Drew *et al.*, GFP-based optimization scheme for the overexpression and purification of eukaryotic membrane proteins in *Saccharomyces cerevisiae*. *Nature Protocols* **3**, 784-798 (2008).
27. I. Zimmermann *et al.*, Synthetic single domain antibodies for the conformational trapping of membrane proteins. *eLife* **7**, (2018).
28. M. Caffrey, V. Cherezov, Crystallizing membrane proteins using lipidic mesophases. *Nature Protocols* **4**, 706-731 (2009).
29. G. Winter, xia2: an expert system for macromolecular crystallography data reduction. *Journal of Applied Crystallography* **43**, 186-190 (2009).
30. G. Winter *et al.*, DIALS: implementation and evaluation of a new integration package. *Acta Crystallogr D Struct Biol* **74**, 85-97 (2018).
31. P. R. Evans, G. N. Murshudov, How good are my data and what is the resolution? *Acta Crystallographica Section D Biological Crystallography* **69**, 1204-1214 (2013).
32. A. J. McCoy *et al.*, Phaser crystallographic software. *Journal of Applied Crystallography* **40**, 658-674 (2007).
33. T. A. Jones, J. Y. Zou, S. W. Cowan, M. Kjeldgaard, Improved methods for building protein models in electron density maps and the location of errors in these models. *Acta crystallographica Section A, Foundations of crystallography* **47 (Pt 2)**, 110-119 (1991).
34. P. Emsley, B. Lohkamp, W. G. Scott, K. Cowtan, Features and development of Coot. *Acta Crystallographica Section D Biological Crystallography* **66**, 486-501 (2010).
35. P. D. Adams *et al.*, PHENIX: a comprehensive Python-based system for macromolecular structure solution. *Acta Crystallographica Section D Biological Crystallography* **66**, 213-221 (2010).

36. E. Blanc *et al.*, Refinement of severely incomplete structures with maximum likelihood in BUSTER-TNT. *Acta Crystallographica Section D Biological Crystallography* **60**, 2210-2221 (2004).
37. J. Schindelin *et al.*, Fiji: an open-source platform for biological-image analysis. *Nat Methods* **9**, 676-682 (2012).